[PS]Pore Characteristics of the Organic-Rich Marine Shales with High Thermal Maturity: A Case Study of the Lower Silurian Longmaxi Gas Shale Reservoirs in Southern China*

Miao Shi[1], Bingsong Yu[2], and Jinchuan Zhang[3]

Search and Discovery Article #51387 (2017)**
Posted June 19, 2017

*Adapted from poster presentation given at AAPG 2017 Annual Convention and Exhibition, Houston, Texas, April 2-5, 2017

[1]School of Energy and Resources, China University of Geosciences, Beijing, China (miaoer727@126.com)
[2]School of Earth Science and Resources, China University of Geosciences, Beijing, China
[3]School of Energy and Resources, China University of Geosciences, Beijing, China

Abstract

The Lower Silurian Longmaxi Formation marine shales, with high organic matter abundance and high thermal maturity, are regarded as the main shale gas reservoirs in China. The pore characteristics of the Longmaxi shales were investigated using samples collected from three investigation wells in southern China. The Longmaxi marine shales are rich in quartz and clay, with average contents of 33.27 wt.% and 32.2 wt.%, respectively. The average TOC content of the samples is 2.32 wt.%, and the average Ro value is 2.4%. Field emission scanning electron microscopy (FESEM), which provides high-resolution images, was used to describe the pore types and structures. Both observation and statistical results indicate that nearly all of the pores are mesopores and macropores, which account for approximately 90% of the total pore volume. Organic matter (OM) pores, interparticle (InterP) pores, and intraparticle (IntraP) pores, are the three main pore types, along with some micro-fracture pores. Typical OM pores within SEM images were extracted by using JMicrovision imaging software and the OM porosity was calculated. OM pores are usually meso- or macropores, and account for a large proportion (approximately 81.4%) of all pores in samples. InterP pores and IntraP pores are often related to rigid particles (quartz, feldspar, or pyrite framboids). Very few InterP or IntraP pores exist between two ductile (clay minerals) particles due to the effects of compaction. Regression analyses suggest that the TOC content is the key factor in pore development for shales with high thermal maturity. The mineral contents (quartz or clay minerals) also contribute to pores development, though their effects are small compared to that of the TOC content. A combination of SEM image analysis, calculations, gas adsorption, and regression analysis shows that the TOC content is the controlling factor for gas storage potential, which infers that OM pores play a pivotal role in high thermal maturity shales, largely determining the gas storage potential. Besides, pores related to rigid particles also provide some space for gas storage, though their effects are extremely small compared to that of the TOC content. Pores related to clay minerals show no significant correlations to gas storage potential under the severe influence of the TOC content.

Reference Cited

Shi, M., B. Yu, Z. Xue, J. Wu, and Y. Yuan, 2015, Pore Characteristics of Organic-Rich Shales with High Thermal Maturity: A Case Study of the Longmaxi Gas Shale Reservoirs from Well Yuye-1 in Southeastern Chongqing, China: Journal of Natural Gas Science and Engineering, v. 26, p. 948-959.

Pore Characteristics of the Organic-Rich Marine Shales With High Thermal Maturity: A Case study of the Lower Silurian Longmaxi Gas Shale Reservoirs in Southern China

Miao Shi*, Bingsong Yu, Jinchuan Zhang
***School of Energy Resources, China University of Geosciences, Beijing 100083, China**
***Email: miaoer727@126.com**

The Lower Silurian Longmaxi Formation marine shales, with high organic matter abundance and high thermal maturity, are regarded as the main shale gas reservoirs in southern China. The pore characteristics of the Longmaxi shales were investigated using samples collected from three investigation wells in southern China. The Longmaxi marine shales are rich in quartz and clay, with average contents of 33.27 wt. % and 32.2 wt. %, respectively. The average TOC content of the samples is 2.32 wt. %, and the average *R*o value is 2.4%.

Image analysis allows us to visualize the pore types and networks in the shale samples. Field emission scanning electron microscopy (FESEM), which provides high-resolution images, was used to describe the pore types and structures. Both observation and statistical results indicate that nearly all of the pores are mesopores (2–50 nm) and macropores (>50 nm), which account for approximately 90% of the total pore volume. Organic matter (OM) pores, interparticle (InterP) pores, and intraparticle (IntraP) pores, are the three main pore types, along with some micro-fracture pores. OM pores, usually meso- or macropores, are the most numerous ones. Typical OM pores within SEM images were extracted by the JMicrovision imaging software. After that, the OM porosity was calculated by the equation $\emptyset = \emptyset_S \frac{V_{OM}}{V_{shale}} = \emptyset_S \frac{\omega_{OM}\rho_{shale}}{\rho_{OM}}$ (Shi et al., 2015) and the result is 1.4%. The average porosity of shale samples is 1.72%. That is, OM pores account for a large proportion (approximately 81.4%) of all pores in samples. However, we suspect that a higher-precision instrument would show that OM pores actually account for an even higher proportion of all pores.

InterP pores and IntraP pores are often related to rigid particles (quartz, feldspar, or pyrite framboids). Very few InterP or IntraP pores exist between two ductile (clay minerals) particles due to the effects of compaction. Regression analyses suggest that the TOC content is the key factor in pore development for shales with high thermal maturity. The mineral contents (quartz or clay minerals) also contribute to pores development, though their effects are small compared to that of the TOC content.

OM pores were formed by the release of hydrocarbon material during OM maturation. Most of the protogenic InterP and IntraP pores were eliminated by severe compaction, and the remains are also diagenetic in origin. A combination of SEM image analysis, calculations, gas adsorption and regression analysis shows that the TOC content is the controlling factor for gas storage potential, which infers that OM pores play a pivotal role in high thermal maturity shales, largely determining the gas storage potential. Besides, pores related to rigid particles also provide some space for gas storage, though their effects are extremely small compared to that of the TOC content. Pores related to clay minerals show no significant correlations to gas storage potential under the severe influence of the TOC content.

Pore Characteristics of the Organic-Rich Marine Shales With High Thermal Maturity: A Case study of the Lower Silurian Longmaxi Gas Shale Reservoirs in Southern China

Miao Shi*, Bingsong Yu, Jinchuan Zhang

***School of Energy Resources, China University of Geosciences, Beijing 100083, China**

***Email: miaoer727@126.com**

Fig. 1 Map of research area and sampling-well locations

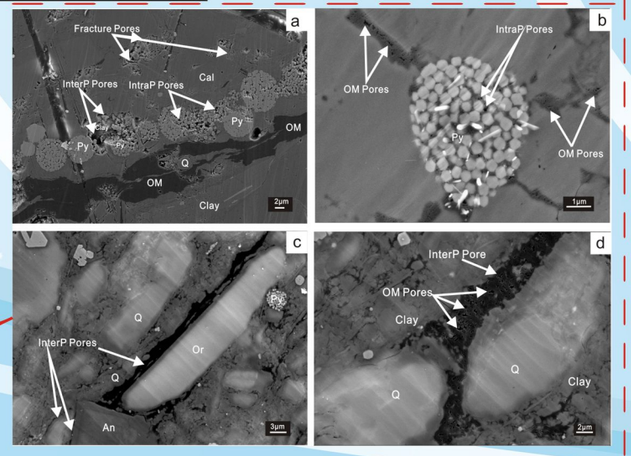

Fig. 2 SEM images of different pore types in the Longmaxi shales (Q-quartz, Py-pyrite, Cal-calcite, Or-orthoclase, An-anorthite)

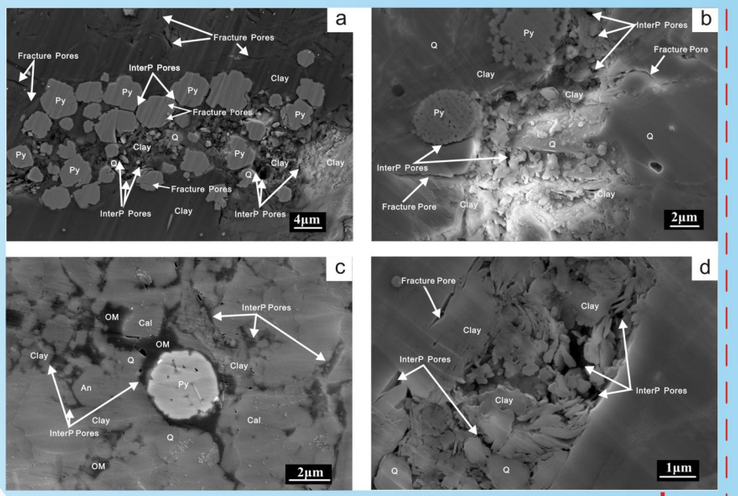

Fig. 3 SEM images of InterP pores (Py-pyrite, Q-quartz, Cal-calcite, An-anorthite)

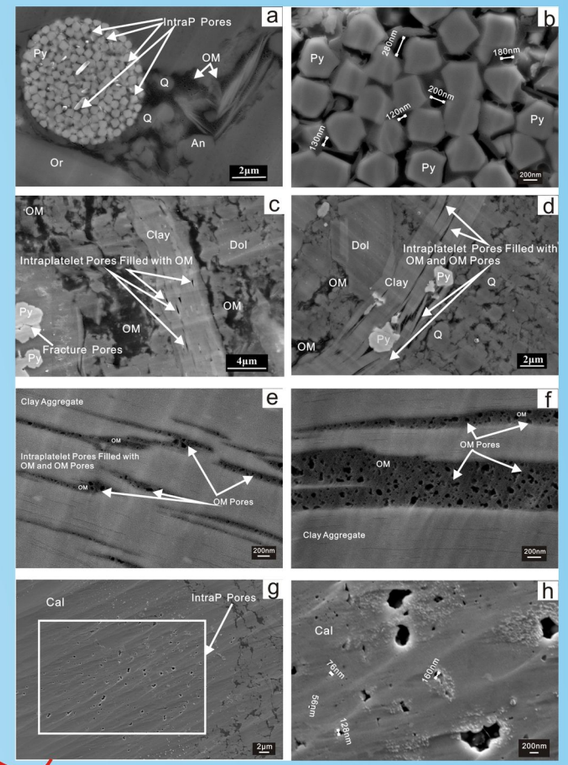

Fig. 4 SEM images of IntraP pores and OM pores (Q-quartz, Dol-dolomite, Py-pyrite, An-anorthite, Cal-calcite)

Pore Characteristics of the Organic-Rich Marine Shales With High Thermal Maturity: A Case study of the Lower Silurian Longmaxi Gas Shale Reservoirs in Southern China

Miao Shi*, Bingsong Yu, Jinchuan Zhang

***School of Energy Resources, China University of Geosciences, Beijing 100083, China**

***Email: miaoer727@126.com**

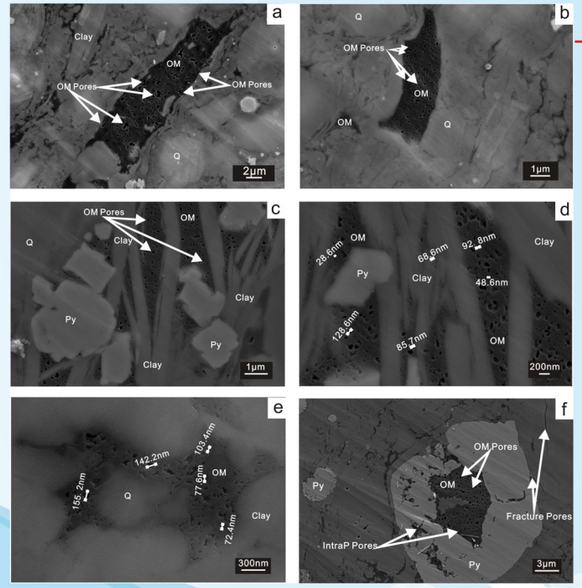

Fig. 5 SEM images of OM pores (Q-quartz, Py-pyrite)

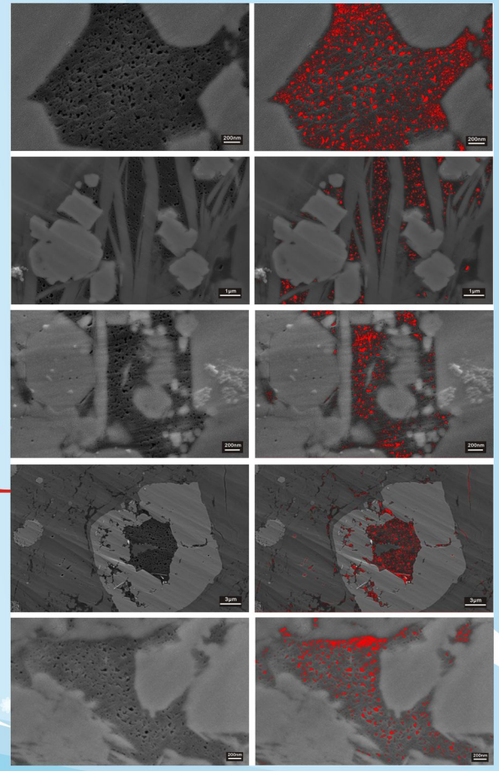

Fig. 6 Examples of the extraction of OM pores

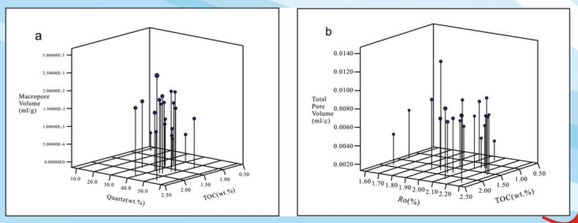

Fig.7 3D graphs relating influencing factors and pore volumes(Well Yuye-1)

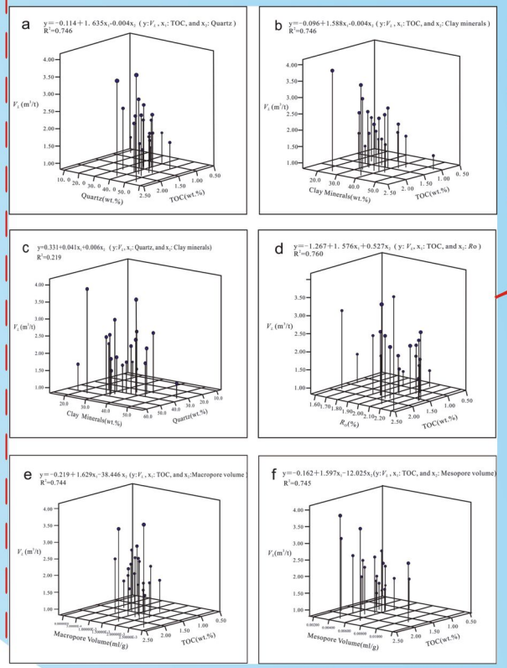

Fig.8 3D graphs relating influencing factors and porosities(Well Xiye-1 and Well Tongye-1)

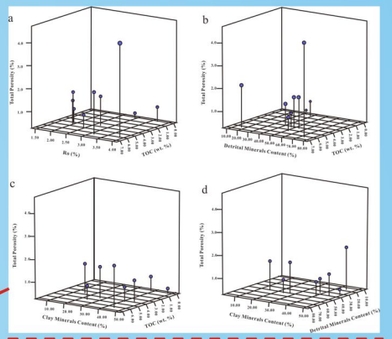

Fig. 9 3D graphs relating influencing factors and saturated adsorption amount(Well Yuye-1)

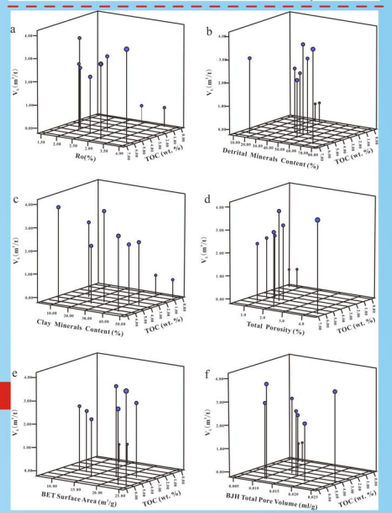

Fig.10 3D graphs relating influencing factors and saturated adsorption amount(Well Xiye-1 and Well Tongye-1)